Circularly polarized high harmonics generated by a bicircular field from inert atomic gases in the *p* state: A tool for exploring chirality-sensitive processes

D. B. Milošević

Faculty of Science, University of Sarajevo, Zmaja od Bosne 35, 71000 Sarajevo, Bosnia and Herzegovina; Academy of Sciences and Arts of Bosnia and Herzegovina, Bistrik 7, Sarajevo, Bosnia and Herzegovina; and Max-Born-Institut, Max-Born-Strasse 2a, 12489 Berlin, Germany

(Received 30 March 2015; revised manuscript received 20 August 2015; published 19 October 2015)

S-matrix theory of high-order harmonic generation (HHG) is generalized to multielectron atoms. In the multielectron case the harmonic power is expressed via a coherent sum of the time-dependent dipoles, while for the one-electron models a corresponding incoherent sum appears. This difference is important for the inert atomic gases having a *p* ground state as used in a recent HHG experiment with a bicircular field [Nat. Photonics **9**, 99 (2015)]. We investigate HHG by such a bicircular field, which consists of two coplanar counter-rotating circularly polarized fields of frequency $r\omega$ and $s\omega$. Selection rules for HHG by a bicircular field are analyzed from the aspects of dynamical symmetry of the system, conservation of the projection of the angular momentum on a fixed quantization axis, and the quantum number of the initial and final atomic ground states. A distinction is made between the selection rules for atoms with closed [J. Phys. B **48**, 171001 (2015)] and nonclosed shells. An asymmetry in emission of the left- and right-circularly polarized harmonics is found and explained by using a semiclassical model and the electron probability currents which are related to a nonzero magnetic quantum number. This asymmetry can be important for the application of such harmonics to the exploration of chirality-sensitive processes and for generation of elliptic or even circular attosecond pulse trains. Such attosecond pulse trains are analyzed for longer wavelengths than in Opt. Lett. **40**, 2381 (2015), and for various field-component intensities.

DOI: 10.1103/PhysRevA.92.043827 PACS number(s): 42.65.Ky, 32.80.Qk, 42.50.Hz, 42.65.Re

I. INTRODUCTION

High-order harmonics generated by a so-called bicircular field have been shown to be a very interesting and useful tool. This field consists of two coplanar counter-rotating circularly polarized fields having different angular frequencies. It was first considered in Refs. [1,2] and was analyzed in detail in Refs. [3,4]. The harmonic-generation efficiency is surprisingly high, only circularly polarized harmonics are generated, and the temporal characteristics of the emitted harmonics are unusual [5]. Very recently, high-order harmonic generation (HHG) by a bicircular field has again attracted attention [6–10] as a source of strong circularly polarized harmonics which can be used for various applications. Angle-resolved electron-energy spectra in strong-field ionization by a bicircular field were analyzed in Ref. [11]. The three-lobed distribution in these spectra has recently been confirmed experimentally [12].

In the previous theoretical investigations of HHG by a bicircular field, a zero-range-potential model [2] and a hydrogen-like-atom model [3–5] were used. For both models the atomic ground state was the *s* state. However, in experiment [1,6,8], multielectron noble-gas atoms with the *p* ground state were used. For this case the above-mentioned theories should be extended. Furthermore, a straightforward generalization of the results obtained by using one-electron models, according to which the *n*th harmonic power P_n is equal to an incoherent sum over *m* of the harmonic powers $P_{n,m}$, which correspond to the atomic state with a fixed magnetic quantum number *m* (for the *p* state the orbital quantum number is $l = 1$ so that $m = 0, \pm 1$), is incorrect. The aim of the present paper is to formulate a theory for an arbitrary (multielectron) ground state and to explore consequences for HHG. We will fill the gap in the present theories and show that, instead of the incoherent sum, a coherent sum of the time-dependent dipoles should be used. Our quantum-mechanical multielectron theory, based on the *S*-matrix formalism, single-active-electron approximation, and the strong-field approximation, is presented in Sec. II and applied to the case of inert atomic gases in *p* states. The selection rules for HHG by a bicircular field are derived in Sec. III. An alternative derivation of the selection rules, based on the dynamical symmetries, is presented in the appendix. Section IV contains our numerical results, while a physical explanation of the observed effects in terms of a semiclassical model, which incorporates the electron probability currents, is given in Sec. V. In Sec. VI we analyze the elliptically polarized attosecond pulse trains for the longer wavelength and different intensities than those used in Ref. [9]. Finally, our conclusions and discussion are given in Sec. VII.

II. *S*-MATRIX THEORY OF HIGH-HARMONIC GENERATION FOR MULTIELECTRON ATOMS

There are various theoretical approaches to HHG [13,14]. Physically, HHG is well described by the three-step model [15]: in the first step the electron is ionized, then it is driven back to the origin by the laser field, and, finally, in the third step, the electron recombines to the ground state and one high-energy photon is emitted. We follow the *S*-matrix approach to HHG [13]. This theory was formulated for one-electron systems, but can be generalized to the *N*-electron atoms considered here, in the sense of the time-dependent Hartree–Fock approximation [16]. The initial and final atomic ground states are presented in the form $|\Psi(t)\rangle = \prod_{j=1}^{N} |\psi_j(t)\rangle$ where $|\psi_j(t)\rangle$ are single-particle orbitals. The *S*-matrix element for the HHG process with

emission of a high harmonic having wave vector $\mathbf{K}$, frequency $\omega_{\mathbf{K}}$, and complex unit polarization vector $\hat{\mathbf{e}}_{\mathbf{K}}$, for an N-electron atom has the form

$$S_{fi} = i \lim_{t'\to\infty} \lim_{t\to-\infty} \langle \Psi_f(t')| \int dt'' G^{(+)}(t',t'') \times c_{\mathbf{K}} \sum_{j=1}^{N} \mathbf{r}_j \cdot \hat{\mathbf{e}}^*_{\mathbf{K}} G^{(+)}(t'',t)|\Psi_i(t)\rangle. \quad (1)$$

This is a straightforward generalization of Eq. (196) from Ref. [13] to multielectron systems. Here $G^{(+)}(t',t'')$ is the Green's operator which corresponds to the total Hamiltonian $H(t) = \sum_{j=1}^{N} H_j(t)$, with the jth-electron Hamiltonian $H_j(t) = -\nabla_j^2/2 + V(\mathbf{r}_j) + \mathbf{r}_j \cdot \mathbf{E}(t)$. The interaction with the laser field, characterized by the electric-field vector $\mathbf{E}(t)$, is taken in the length gauge and dipole approximation and the atomic system of units is used. The operator of the jth electron coordinate $\mathbf{r}_j$ acts as a unit operator in the subspaces of other electrons, i.e., $\mathbf{r}_j \equiv \prod_{i=1}^{j-1} \mathbf{1}_i \bigotimes \mathbf{r}_j \bigotimes \prod_{k=j+1}^{N} \mathbf{1}_k$. We also introduce the states $|\Phi_j^{(\pm)}(t)\rangle$ which satisfy the time-dependent Schrödinger equation

$$\left[i\frac{\partial}{\partial t} - H(t) \right] |\Phi_j^{(\pm)}(t)\rangle = 0, \quad j = i, f, \quad (2)$$

and the field-free boundary conditions

$$\begin{aligned} i \lim_{t'\to\infty} \langle \Psi_f(t')|G^{(+)}(t',t'') &= \langle \Phi_f^{(-)}(t'')|, \\ i \lim_{t\to-\infty} G^{(+)}(t'',t)|\Psi_i(t)\rangle &= |\Phi_i^{(+)}(t'')\rangle, \end{aligned} \quad (3)$$

so that the S-matrix element (1) can be rewritten as

$$S_{fi} = -ic_{\mathbf{K}} \int_{-\infty}^{\infty} dt e^{i\omega_{\mathbf{K}} t} \hat{\mathbf{e}}^*_{\mathbf{K}} \cdot \mathbf{d}_{fi}(t), \quad (4)$$

where $\mathbf{d}_{fi}(t)$ is the time-dependent dipole matrix element between the initial and final laser-dressed states

$$\mathbf{d}_{fi}(t) = \langle \Phi_f^{(-)}(t)| \sum_j \mathbf{r}_j |\Phi_i^{(+)}(t)\rangle. \quad (5)$$

Analogously as in Ref. [13], power (intensity) of the nth harmonic irradiated in the direction of the z-axis unit vector $\hat{\mathbf{e}}_z$, for a laser electric-field vector $\mathbf{E}(t)$ with the period T and frequency $\omega = 2\pi/T$, is defined by

$$P_n = \frac{(n\omega)^4}{2\pi c^3} |T_n|^2, \quad (6)$$

where $T_n = \hat{\mathbf{e}}_n^* \cdot \mathbf{T}_n$ is the T-matrix element for transition from the initial to the final state, with $\hat{\mathbf{e}}_n = \hat{\mathbf{e}}_{\mathbf{K}}$ being the nth harmonic photon unit complex polarization vector, and

$$\mathbf{T}_n = \int_0^T \frac{dt}{T} \mathbf{d}_{fi}(t) e^{in\omega t} = T_n \hat{\mathbf{e}}_n = T_n^x \hat{\mathbf{e}}_x + T_n^y \hat{\mathbf{e}}_y \quad (7)$$

is the Fourier component of the time-dependent dipole matrix element $\mathbf{d}_{fi}(t)$ [Eq. (5)]. Within the strong-field approximation, the time-dependent dipole can be approximated by

$$\mathbf{d}_{fi}(t) \approx \langle \Psi_f(t)| \sum_j \mathbf{r}_j \int dt' G^{(+)}(t,t') \sum_k \mathbf{r}_k \cdot \mathbf{E}(t')|\Psi_i(t')\rangle, \quad (8)$$

where the Green's operator $G^{(+)}$ is a direct product of the single-electron Green's operators $G_j^{(+)} \equiv \prod_{i=1}^{j-1} \mathbf{1}_i \bigotimes G_j^{(+)} \bigotimes \prod_{k=j+1}^{N} \mathbf{1}_k$. Within the single-active-electron approximation only one electron is propagated so that $G^{(+)} \approx \sum_j G_j^{(+)}$. We suppose that, in Eq. (8), only the terms with $k = j$ contribute to the HHG process, i.e., the same jth electron is ionized via the interaction $\mathbf{r}_j \cdot \mathbf{E}(t')$, propagates in the laser field by the propagator $G_j^{(+)}$, and, during recombination, emits a high harmonics via the interaction $\hat{\mathbf{e}}^*_{\mathbf{K}} \cdot \mathbf{r}_j$. Denoting this active electron with the index a, we obtain

$$\begin{aligned} \mathbf{d}_{fi}^{(a)}(t) &= \langle \psi_{af}(t)|\mathbf{r}_a \int dt' G_a^{(+)}(t,t') \mathbf{r}_a \cdot \mathbf{E}(t')|\psi_{ai}(t')\rangle, \\ \mathbf{d}_{fi}(t) &\approx \sum_a \mathbf{d}_{fi}^{(a)}(t). \end{aligned} \quad (9)$$

Here, i and f denote the initial and final states of the ath electron. The wave vectors $|\psi_{aj}(t)\rangle = |\psi_{aj}\rangle \exp(-iE_j t)$, $j = i, f$, are determined by the states $|\psi_{aj}\rangle$ and the energies E_j, which are the solutions of the laser-free stationary Schrödinger equation. In the strong-field approximation, dominant is the contribution of the dipole [13]

$$\mathbf{d}_{fi}^{(a)}(t) \approx -i\left(\frac{2\pi}{i}\right)^{3/2} \int_0^{\infty} \frac{d\tau}{\tau^{3/2}} \langle \psi_{af}|\mathbf{r}_a|\mathbf{k}_s + \mathbf{A}(t)\rangle \times \langle \mathbf{k}_s + \mathbf{A}(t-\tau)|\mathbf{r}_a \cdot \mathbf{E}(t-\tau)|\psi_{ai}\rangle e^{iS_s}, \quad (10)$$

where $\mathbf{A}(t) = -\int^t dt' \mathbf{E}(t')$, $\mathbf{k}_s \equiv \int_t^{t-\tau} dt' \mathbf{A}(t')/\tau$ is the stationary momentum, and $S_s \equiv E_f t - \int_{t-\tau}^{t} dt' [\mathbf{k}_s + \mathbf{A}(t')]^2/2 - E_i(t-\tau)$ is the action.

We model the ground-state atomic wave function by a linear combination of the Slater-type orbitals $\psi_{n_a lm}(\mathbf{r}) \propto r^{n_a - 1} e^{-\zeta_a r} Y_{lm}(\hat{\mathbf{r}})$, obtained by using the Hartree–Fock–Roothaan method [17]. Let us now apply the above result to the atoms having the p ground state (generalization to an arbitrary ground state is straightforward but, having in mind an application to the generation of circularly polarized harmonics, we consider only this case in the present paper). For the p ground state the magnetic quantum number is $m = 0, \pm 1$. The initial (final) state is characterized only by the quantum number m_i (m_f). For atoms with closed electron shells (Ne, Ar, Kr, Xe) the m-changing transitions are forbidden by the Pauli exclusion principle. Namely, for an outer electron configuration np^6 the electron emitted initially from an m_i state cannot end up in $m_f \neq m_i$ state since these states are occupied by other np electrons. Since we neglect the influence of the spin (i.e., we consider that the pairs of electrons with the spin $m_s = \pm 1/2$ from the np^6 configuration interact with the laser field in the same way), only three electrons are active, and we have

$$\mathbf{d}_{fi}(t) \approx \sum_{a=1,2,3} \mathbf{d}_{fi}^{(a)}(t)_{|m_i = m_f = m} = \sum_m \mathbf{d}_m(t), \quad (11)$$

where $\mathbf{d}_m(t)$ ($m = 0, \pm 1$) is given by Eq. (10) with $\psi_{aj}(\mathbf{r}_a) \propto Y_{lm_j}(\hat{\mathbf{r}}_a)$, $j = i, f$, and $E_f = E_i = -I_p$ with I_p being the ionization potential. The matrix elements in Eq. (10) can be calculated analytically taking into account that $\langle \mathbf{q}|\mathbf{r}|\psi_{n_a lm}\rangle = i\partial\tilde{\psi}_{n_a lm}(\mathbf{q})/\partial\mathbf{q}$, where $|\mathbf{q}\rangle$ is a plane wave, $\tilde{\psi}_{n_a lm}(\mathbf{q})$ are the Slater-type orbitals in the momentum space, and, in spherical coordinates, $\partial/\partial\mathbf{q} = \hat{\mathbf{e}}_q \partial/\partial q + \hat{\mathbf{e}}_{\theta_q} q^{-1} \partial/\partial\theta_q +$

$\hat{\mathbf{e}}_{\phi_q}(q\sin\theta_q)^{-1}\partial/\partial\phi_q$. Our bicircular field is defined in the xy plane so that the vector $\mathbf{q}$ lies in the same plane. Then, for the z axis as the quantization axis, we have $\theta_q = 90^\circ$ and the Descartes (q_x,q_y,q_z) components of the unit vectors are $\hat{\mathbf{e}}_q = (\cos\phi_q, \sin\phi_q, 0)$, $\hat{\mathbf{e}}_{\theta_q} = (0,0,-1)$, $\hat{\mathbf{e}}_{\phi_q} = (-\sin\phi_q, \cos\phi_q, 0)$. Since $\theta_q = 90^\circ$ and $\hat{\mathbf{e}}_x \cdot \hat{\mathbf{e}}_{\theta_q} = \hat{\mathbf{e}}_y \cdot \hat{\mathbf{e}}_{\theta_q} = 0$, it can be shown that $\langle \mathbf{q}|\mathbf{r}\cdot\mathbf{E}(t)|\psi_{n_a 10}\rangle = 0$, i.e., only the wave functions with $m = \pm 1$ contribute to the harmonic emission. For Ne atoms having the $2p$ ground state, the corresponding matrix elements are given by $\langle \mathbf{q}|\mathbf{r}\cdot\hat{\mathbf{e}}_x|\psi_{21\pm1}\rangle = c_a(q)[\pm 6q_x q_\pm \mp (q^2+\zeta_a^2)]$, $\langle \mathbf{q}|\mathbf{r}\cdot\hat{\mathbf{e}}_y|\psi_{21\pm1}\rangle = c_a(q)[\pm 6q_y q_\pm - i(q^2+\zeta_a^2)]$, with $c_a(q) = 8\zeta_a^{7/2}/[\pi(q^2+\zeta_a^2)^4]$, $q_\pm = q_x \pm iq_y$. We obtained similar simple analytical results for other inert gases. This enables fast numerical calculations. For an arbitrarily oriented axis of quantization defined by the Euler angles α,β,γ and the rotation matrix $D^l(\alpha\beta\gamma)$, we have [18] $Y_{lm}(\hat{\mathbf{r}}') = \sum_{m'} D^l_{m'm}(\alpha\beta\gamma)Y_{lm'}(\hat{\mathbf{r}})$. In the T matrix we have a product of matrix elements summed over all m so that, by using the orthonormality relation $\sum_m D^{l*}_{m'm}(\alpha\beta\gamma)D^l_{m''m}(\alpha\beta\gamma) = \delta_{m'm''}$, we get that T_n does not depend on the choice of quantization axis.

Let us summarize our results obtained applying the multielectron S-matrix approach within the single-active-electron approximation and the strong-field approximation to inert atomic gases with a p ground state. Since the initial and final multielectron states are the same, the sum over the final states and averaging over the initial states gives only one term P_n which is given by Eqs. (6), (7), and (11) with (10). However, in the one-electron theory, formulated in our previous publications, the nth harmonic power, summed over all final states and averaged over all initial states, is given by

$$P_n^{(1e)} = \frac{(n\omega)^4}{2\pi c^3}\frac{1}{2l+1}\sum_{m_i,m_f}\left|\int_0^T \frac{dt}{T}\mathbf{d}_{fi}^{(1e)}(t)e^{in\omega t}\right|^2, \quad (12)$$

where $\mathbf{d}_{fi}^{(1e)}(t)$ is the (one-term) time-dependent dipole matrix element for the transition from the initial state m_i to the final state m_f, which is given by Eq. (10). The result (12) is obviously different from the result (11), which is obtained by using the theory formulated in the present paper. In the case of the s ground state we have $m_i = m_f = 0$ and the old and new theories give the same result.

III. SELECTION RULES FOR THE BICIRCULAR FIELD

A bicircular laser field is a bichromatic circularly polarized field with counter-rotating components having the angular frequencies $r\omega$ and $s\omega$, which are integer multiples of the same fundamental frequency ω. The corresponding electric-field vector is defined by [3–5]

$$\mathbf{E}(t) = \frac{i}{2}(E_1\hat{\mathbf{e}}_+ e^{-ir\omega t} + E_2\hat{\mathbf{e}}_- e^{-is\omega t}) + \text{c.c.}, \quad (13)$$

where $\hat{\mathbf{e}}_\pm = (\hat{\mathbf{e}}_x \pm i\hat{\mathbf{e}}_y)/\sqrt{2}$ and E_j and $I_j = E_j^2$ are the electric-field vector amplitude and intensity of the jth field component of helicity h_j ($h_1 = 1$, $h_2 = -1$). It was shown in Ref. [4] that the harmonics generated by the field (13) are circularly polarized and that only those harmonics of order n and ellipticity ε_n are emitted which satisfy the following selection rule:

$$\varepsilon_n = \pm 1 \quad \text{for} \quad n = q(r+s) \pm r, \quad (14)$$

where q is an integer.

A general derivation of this selection rule based on dynamical symmetries is given in the appendix. We now derive this selection rule in a simpler way: by supposing that the quantization axis of the ground state is the z axis, so that the projections of the angular momentum on the z axis are $m_i, m_f = 0, \pm 1$. In the HHG process, the changes of the angular momentum projection are

$$\begin{aligned}\Delta J_{z,\text{atom}} &= m_i - m_f,\\ \Delta J_{z,\text{laser}} &= \Delta n_r(+1) + \Delta n_s(-1),\\ \Delta J_{z,\text{harmonic}} &= -\varepsilon_n,\end{aligned} \quad (15)$$

where Δn_r (Δn_s) is the difference between the number of absorbed and emitted laser photons of frequency $r\omega$ ($s\omega$) and the "$-$" sign on the right-hand side of last equation is because one harmonic photon of helicity $\varepsilon_n = \pm 1$ is emitted. The conserving condition for the angular momentum projection leads to

$$\sum \Delta J_z = 0 \Rightarrow m_i - m_f + \Delta n_r - \Delta n_s - \varepsilon_n = 0, \quad (16)$$

while the energy-conserving condition for the nth-harmonic energy gives

$$n\omega = \Delta n_r r\omega + \Delta n_s s\omega. \quad (17)$$

With the notation $q = \Delta n_s$, from the last two equations we obtain $n\omega = (q + \varepsilon_n + m_f - m_i)r\omega + qs\omega$. For $\varepsilon_n = \pm 1$ we have

$$n\omega = q(r+s)\omega + (m_f - m_i \pm 1)r\omega, \quad (18)$$

which is a general result. For the s ground states it is $m_i = m_f = 0$ and we obtain $n\omega = q(r+s)\omega \pm r\omega$. For a p ground state, with the quantization axis chosen to be along the z axis and with the closed shell, it is $m_i = m_f$ (the m-changing transitions are forbidden by the Pauli exclusion principle) and we obtain the same selection rule, which is in agreement with the experiment and the result (14). An analogous selection rule for HHG by a bichromatic elliptically polarized field is derived in Ref. [10].

If the shell is not closed, then it is possible that $m_i \neq m_f$ [19]. If the dipole matrix element for $m = 0$ is equal to zero, then only the cases $m_i = \pm 1$, $m_f = \pm 1$ are possible. The case $m_f = m_i = \pm 1$ is already included in the selection rule (14), while the case $m_f = -m_i = \pm 1$, due to $m_f - m_i \pm 1 = 2m_f \pm 1$ (for $m_f = 1$ it is $2m_f + 1 = 3$ and $2m_f - 1 = 1$, while for $m_f = -1$ we have $2m_f + 1 = -1$ and $2m_f - 1 = -3$), leads to a generalized selection rule (valid for the nonclosed shells):

$$n\omega = q(r+s)\omega \pm v r\omega, \quad v = 1,3. \quad (19)$$

For $r = 1$ and $s = 2$ the harmonics $n = 3q \pm 1$ and $n = 3q \pm 3$ are emitted, which means that all harmonics $n = 1,2,3,\ldots$ can be emitted and, in general, they are elliptically polarized. For example, for $v = 3$ there are two contributions to the harmonic $n = 9$, with the helicities $\varepsilon_9 = 1$ (for $q = 2$ and the "$+$" sign) and $\varepsilon_9 = -1$ (for $q = 4$ and the "$-$" sign), which

add coherently, so that the harmonic $n = 9$ is elliptically polarized and its ellipticity depends on the relative contributions of the two corresponding harmonic strengths. By using the selection rule (19), it can be shown that, for $r = 1$ and $s = 3$, all harmonics are odd. For $r = 1$ and $s = 4$ all harmonics except the harmonics $5q$, with q an integer, are emitted, etc.

IV. NUMERICAL RESULTS FOR THE HIGH-HARMONIC-GENERATION SPECTRA

In order to illustrate our theory and to elucidate the physics behind it, we choose the example of Ne atoms with the $2p$ ground state and the bicircular field (13) with $r = 1$ and $s = 2$. In Fig. 1 we present the harmonic intensity as a function of the harmonic order for Ne atoms modeled by using the hydrogen-like-atom model with the s ground state [black solid curve in Fig. 1(a)] and by the realistic $2p$ state with four orbitals [17] (all other curves). The inset in Fig. 1(a) shows our bicircular field obtained by combining the ω and 2ω fields having the same intensities and the helicity $+1$ and -1, respectively. The position of the harmonic cutoff at $n = 212$ is obtained using the semiclassical three-step model described in Ref. [3]. For the model with the s ground state the intensities of the harmonics $n = 3q + 1$ and $n = 3q - 1$, having the opposite helicities, are comparable, so that the curve of the corresponding spectrum is continuous. However, for the $2p$ ground state the intensities of the harmonics $n = 3q - 1$, having the ellipticity $\varepsilon_n = -1$, are different from that of the harmonics $n = 3q + 1$, for which $\varepsilon_n = 1$. For low harmonics ($30 < n < 64$) the harmonics with $\varepsilon_n = 1$ are stronger, but for the plateau and cutoff harmonics, which are of our interest here, the $\varepsilon_n = -1$ harmonics are stronger by up to five times. Similar results, for a shorter fundamental wavelength of 800 nm were presented in Ref. [9]. For the presently used fundamental wavelength of 1300 nm, the harmonic-photon-energy region with a significant asymmetry between the $\varepsilon_n = 1$ and $\varepsilon_n = -1$ harmonics is much wider ($45 < n < 63$ for 800 nm from Ref. [9] vs $100 < n < 212$ for 1300 nm), so that the shorter elliptically polarized attosecond pulse trains can be generated (see Sec. VI).

The partial spectra for particular values $m = m_i = m_f = -1$ and $m_i = m_f = +1$ are shown in Figs. 1(b) and 1(c), respectively. The asymmetry between the $\varepsilon_n = -1$ and $\varepsilon_n = 1$ harmonics is now stronger. The strongest are the harmonics for $m = -1$ and $\varepsilon_n = -1$. In the plateau and cutoff region they are up to two orders of magnitude stronger than the weakest harmonics having $m = 1$ and $\varepsilon_n = -1$. One can also notice that, for $m = -1$ stronger are the $\varepsilon_n = -1$ harmonics, while for $m = 1$ the situation is opposite: the $\varepsilon_n = 1$ harmonics are more intense. We also calculated the harmonic spectra for a counter-rotating bicircular field having the opposite helicity of the components ($h_1 = -1$, $h_2 = 1$). In this case, the spectrum for the s state remains unchanged, while the $\varepsilon_n = 1$ and $\varepsilon_n = -1$ spectra for the p state from Fig. 1(a) interchange. Analogously, for Figs. 1(b) and 1(c) we have the symmetry $(m = -1, \varepsilon_n = \pm 1) \leftrightarrow (m = 1, \varepsilon_n = \mp 1)$ for $(h_1, h_2) \leftrightarrow (-h_1, -h_2)$.

Finally, in Figs. 1(b) and 1(c) we also explore the influence of the intensity of the bicircular-field components on the HHG spectra. One can notice that the mentioned asymmetry in emission of harmonics having opposite helicities does not

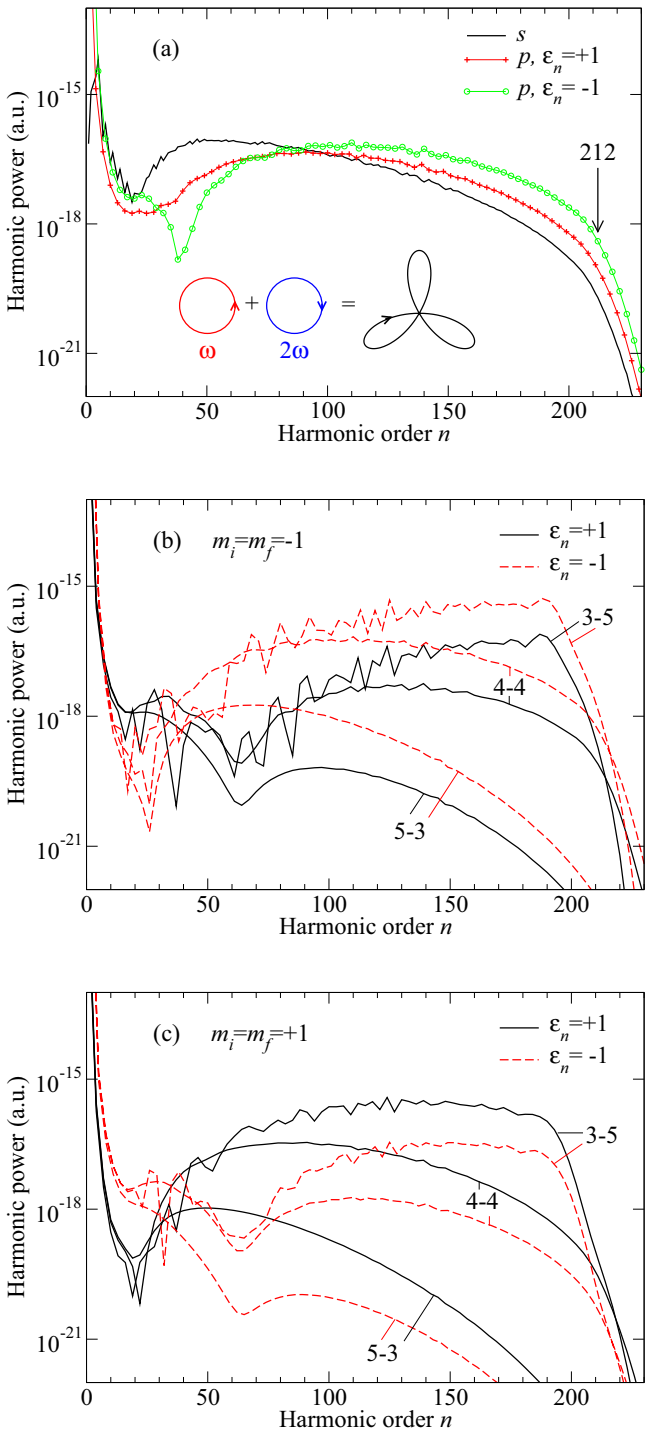

FIG. 1. (Color online) Harmonic power as a function of the harmonic order for HHG by bicircular field for Ne atoms and the field-component wavelengths $\lambda_1 = 1300$ nm and $\lambda_2 = 650$ nm and intensities expressed in multiples of 10^{14} W/cm^2 and denoted by $j_1 - j_2$, where $j_1, j_2 = 3,4,5$. The nth harmonic ellipticity is $\varepsilon_n = \pm 1$ for $n = 3q \pm 1$, q integer. (a) Comparison of the results obtained by using the realistic $2p$ ground state and by using the hydrogen-like-atom model with the s ground state. The laser intensities of the components equal 4×10^{14} W/cm^2 ($j_1 = j_2 = 4$). The cutoff at $n = 212$ is also denoted. (b), (c) The results obtained for $j_1, j_2 = 3,4,5$ are presented for the values of the initial- and final-state magnetic quantum numbers m_i and m_f as denoted.

change much with the change of the components' relative intensities. However, the plateau and the cutoff harmonics are much stronger (up to five orders of magnitude) for the higher 2ω-field component intensity.

V. SEMICLASSICAL THREE-STEP MODEL AND ELECTRON PROBABILITY CURRENTS

HHG due to bicircular fields was described very well by using the semiclassical three-step model in Ref. [3]. In order to understand the above-described behavior of the HHG spectra for the p ground states, we use this model and the fact that the electron probability current for the p ground state is proportional to the magnetic quantum number m. For the explanation we use Fig. 2 in which we present the electric-field vector, vector potential, and the dominant electron trajectory and velocity, obtained by using the quantum-orbit theory [20].

In the left panels of Fig. 2 we show the electric-field vector and the vector potential of the bicircular field used in Fig. 1(a). The field at the ionization and recombination times, which correspond to the dominant quantum orbit for the emission of the cutoff harmonic $n = 212$, is denoted by I and R, respectively. Between the ionization and recombination the field is almost linearly polarized [21], having a small negative value of E_y. The drift electron momentum, measured at the detector, in the above-threshold ionization [11,20] is in the direction close to the negative x axis which is opposite to the vector potential direction at the ionization time. At the recombination time both components of the vector potential are maximal, which leads to a maximum harmonic photon energy.

In the right-hand panels of Fig. 2 we present the dominant electron trajectory and velocity, which are obtained by using

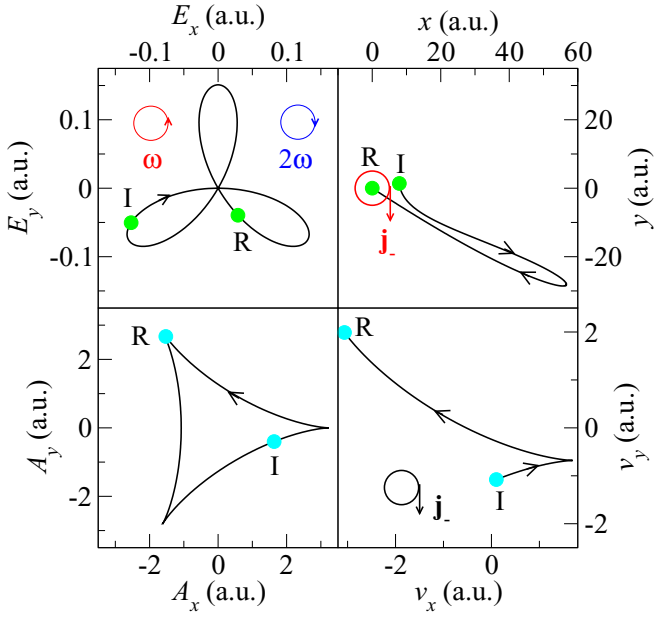

FIG. 2. (Color online) The $\omega-2\omega$ bicircular electric field vector (upper-left panel), vector potential (lower left), and electron trajectory (upper right) and velocity (lower right) between the ionization (I) and recombination (R) times which correspond to the cutoff harmonic $n = 212$. The relevant electron probability current $\mathbf{j}_-$ is shown in the right-hand panels.

the semiclassical three-step model [3] and correspond to the emission of the cutoff harmonic $n = 212$. The electron is born at the time $t_{\rm ion}$ at the end of tunnel about 8 a.u. from the origin and starts to move in the negative y direction. The corresponding velocity starts from a small negative value of the v_y component [22]. This small $v_y(t_{\rm ion})$ is necessary to compensate the small value of the E_y component in order that the electron can return to the origin and recombine in the HHG process. For $t > t_{\rm ion}$, under the action of the force $\mathbf{F}(t) = -\mathbf{E}(t)$, both velocity components increase. The x component of the electric field changes its sign at the point $\mathbf{E}(0) = \mathbf{0}$ so that the electron's velocity component v_x starts to decrease, while the component v_y keeps increasing, up to the recombination time when both v_y and $|v_x|$ have maxima leading to a maximum harmonic photon energy.

In order to be able to return to the parent ion and recombine with it in the HHG process, the electron has to have an initial velocity $v_y(t_{\rm ion}) < 0$. According to the semiclassical model of Ref. [3], the probability that the electron has large $|v_y(t_{\rm ion})|$ is low and, consequently, the corresponding harmonic intensity is low. We have seen that [see Fig. 1(b) in Ref. [9] and Figs. 1(b) and 1(c) here] that, for the atomic ground state with the magnetic quantum number $m = -1$, the intensity of the plateau and cutoff harmonics is higher. This means that it is more probable that $|v_y(t_{\rm ion})|$ has a large value for the ionization from the $m = -1$ ground state than for the ionization from the $m = +1$ state. It is known [23] that, for atomic orbitals having $m \neq 0$, the electric ring current exist, whose direction is determined by the sign of m. In the spherical coordinates (with $\theta = 90^\circ$ in our case) the corresponding electric probability current density in the state $\psi_{n_a lm}$ is

$$\mathbf{j}_m = m|\psi_{n_a lm}|^2 \frac{\hat{\mathbf{e}}_\varphi}{r}. \tag{20}$$

For $m = -1$ this current is shown in the right-hand panels of Fig. 2. Since $x(t_{\rm ion})$ is positive, the y component of $\mathbf{j}_m$ is negative for $m = -1$ and it is more probable that the electron appears with large $|v_y(t_{\rm ion})|$ [$v_y(t_{\rm ion}) < 0$] than in the $m = +1$ case. This explains why the harmonic intensity for $m = -1$ in Fig. 1 is higher.

In addition to this, for $m = \pm 1$ the recombination is such that the harmonics having $\varepsilon_n = \pm 1$ are stronger, i.e., the recombination is more probable if the bound m state is corotating with the circular field of the emitted harmonics. This is also in accordance with the results of Fig. 1. That the recombination for corotating case is more probable follows from the fact that the recombination matrix element is the complex conjugate of the photoionization matrix element and the known result that one-photon ionization by a circularly polarized field which co-rotate with the bound state is more probable [24].

VI. GENERATION OF ELLIPTICALLY POLARIZED ATTOSECOND PULSE TRAINS

In Ref. [9] we showed that, by using a group of high harmonics generated by exposing atoms with the p ground state to a bicircular field, it is possible to generate elliptically polarized attosecond pulse trains. In the present paper we have shown that, by using a longer wavelength, it is

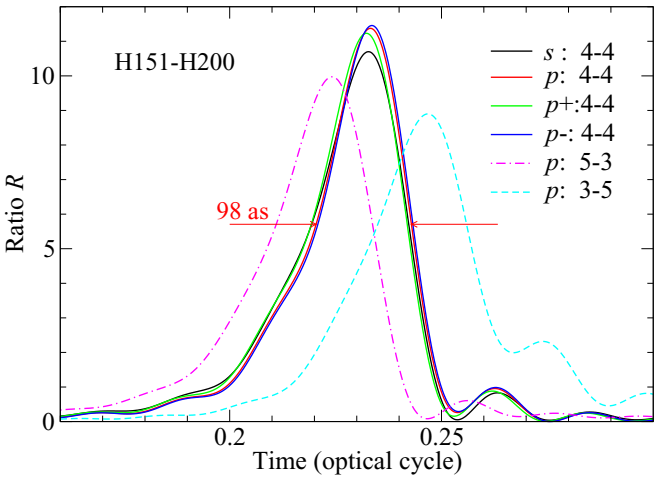

FIG. 3. (Color online) Ratio of the coherent to incoherent harmonic intensities as a function of the time expressed in optical cycles T. The results for the groups of harmonics having the ellipticity $\varepsilon_n = +1$ ($n = 151,154,\ldots,196,199$) and $\varepsilon_n = -1$ ($n = 152,155,\ldots,197,200$) are presented. For the curves denoted by s (black curve; s ground state) and p (red curve; $2p$ ground state) all harmonics are taken into account, while for the green (blue) curve denoted by $p+$ ($p-$) only the harmonics having the ellipticity $\varepsilon_n = +1$ ($\varepsilon_n = -1$) are included. The laser and atomic parameters are as in Fig. 1. The laser component intensities are $I_i = j_i \times 10^{14}$ W/cm^2 ($i = 1,2$), where $j_1 = j_2 = 4$ for all curves except for the magenta dot-dashed curve for which $j_1 = 5$ and $j_2 = 3$ and the cyan dashed curve for which $j_1 = 3$ and $j_2 = 5$ (for these two curves the ground state is $2p$ and all harmonics are taken into account).

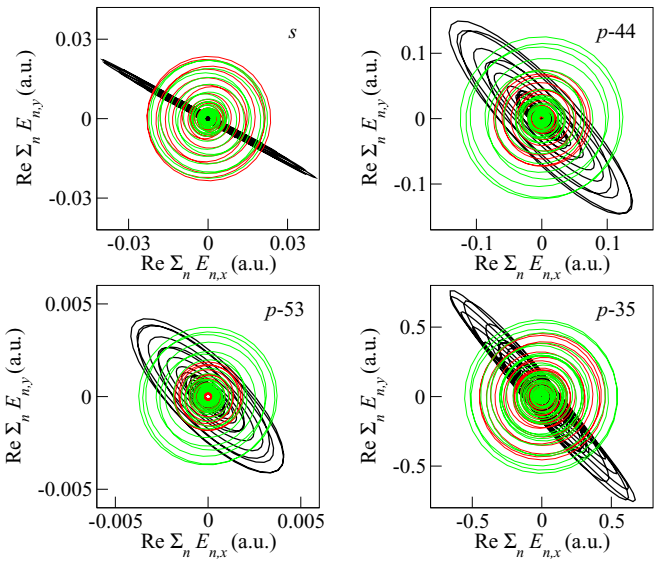

FIG. 4. (Color online) Electric-field vector of a group of harmonics ($n = 151,152,\ldots,199,200$) during one-third of the cycle of the driving field. In each panel three traces are shown: all harmonics (black bold lines), all harmonics having the ellipticity $\varepsilon_n = +1$ (red curves), and all harmonics having the ellipticity $\varepsilon_n = -1$ (green curves). In the upper-left panel, the results obtained by using the s ground state are shown, while for the remaining three panels, the p ground state is used for the following intensities of the bicircular-field components: $I_1 = I_2 = 4 \times 10^{14}$ W/cm^2 (upper panels), $I_1 = 5 \times 10^{14}$ W/cm^2 and $I_2 = 3 \times 10^{14}$ W/cm^2 (lower-left panel), and $I_1 = 3 \times 10^{14}$ W/cm^2 and $I_2 = 5 \times 10^{14}$ W/cm^2 (lower-right panel). The other laser and atomic parameters are as in Fig. 1.

possible to obtain a longer plateau, which consists of more harmonics that show an asymmetry with respect to their helicity. In order to explore the consequences of this effect on the mentioned generation of the attosecond pulse trains, as in Refs. [5,9], we introduce the complex time-dependent nth harmonic electric-field vector $\mathbf{E}_n(t) = n^2\mathbf{T}_n \exp(-in\omega t)$, where t is the harmonic emission time, and consider the field formed by a group $\mathcal{N}$ of subsequent harmonics. We calculate the ratio of the coherent to incoherent sum of harmonic intensities $R(\mathcal{N};t) = |\sum_{\mathcal{N}} \mathbf{E}_n(t)|^2 / \sum_{\mathcal{N}} |\mathbf{E}_n(t)|^2$. In Fig. 3 we present this ratio for a group of plateau and cutoff harmonics $\mathcal{N} = \{151,152,\ldots,199,200\} = \mathcal{N}_+ \bigcup \mathcal{N}_-$, where the groups of harmonics $\mathcal{N}_\pm$ have the helicity $\varepsilon_n = \pm 1$ and $\mathcal{N}_+ = \{151,154,\ldots,196,199\}$ and $\mathcal{N}_- = \{152,155,\ldots,197,200\}$. We separately show the results obtained by using the s and p ground states. For the p ground state we also present by different curves (denoted by $p\pm$) the results for the groups of harmonics $\mathcal{N}_\pm$ and the results for different intensities of the bicircular-field components as denoted in the figure. In all cases we have an attosecond pulse which repeats three time within one cycle of the driving field. Only one pulse is shown in Fig. 3 for better visibility. The full width at half maximum (FWHM) for all pulses is $\lesssim$100 as. The presented results are similar to those from Ref. [9]. The difference is that the ratio R is more than two times larger for the 1300 nm driving laser field used in the present paper. The FWHM of each pulse is now shorter (98 as) compared to 150 as from Ref. [9] for 800 nm.

In Fig. 4 we present the electric-field vector for one-third of the driving field optical cycle of the groups of harmonics $\mathcal{N}$ (black curves), $\mathcal{N}_+$ (red curves), and $\mathcal{N}_-$ (green curves). The presented field for the s ground state is approximately linearly polarized. If we present the parametric plot of this field for the full optical cycle T, then we obtain a star-like structure that has a threefold symmetry which reflects the threefold symmetry of the driving field. The strengths of the corresponding fields for the harmonics having ellipticity $\varepsilon_n = +1$ (red line) and $\varepsilon_n = -1$ (green line) are approximately equal so that the corresponding red and green smooth circular traces cover the same area of the polar plot. On the other hand, for the p ground state, the above linear structure becomes elliptical, as can be seen in the remaining panels of Fig. 4. The ellipticity of the presented field is higher for the higher intensity of the ω component of the driving field. For the higher intensity of the 2ω component (lower-right panel) the ellipticity is smaller but the corresponding field strength is much higher (three orders of magnitude).

VII. CONCLUSIONS AND DISCUSSION

In conclusion, we presented a general theory of HHG by multielectron atoms, which is based on the S-matrix formalism, single-active-electron approximation, and the strong-field approximation. We applied this theory to HHG by a bicircular field having frequencies $r\omega$ and $s\omega$ (r,s are integers). By choosing the quantization axis for atomic system to be perpendicular to the polarization plane of the bicircular field, we derived general selection rules. For inert atomic gases having the p ground state we found a strong asymmetry

in emission of left- and right-circularly polarized high harmonics. We explained this asymmetry by incorporating the electron probability current corresponding to the magnetic quantum number m into the semiclassical three-step model of Ref. [3].

From the practical point of view, the asymmetry in emission of the circularly polarized high-order harmonics having opposite helicities ($\varepsilon_n = \pm 1$) is important in many aspects. In particular, it is important for investigating the chirality-sensitive properties of light-matter interactions. Examples are photoelectron circular dichroism in chiral molecules [25] and x-ray magnetic circular dichroism spectroscopy [26]. Up to now, such radiation has only been available at large-scale x-ray facilities such as synchrotrons. The advantages of the circular high harmonics is that they offer a table-top soft-x-ray source of coherent light.

By phase locking a group of high harmonics it is possible to generate a train of attosecond pulses [27]. For the s ground state of an atom, the polarization of the generated pulse trains is close to linear [5]. However, for the p ground state, due to the above-mentioned asymmetry, this polarization is elliptic and even close to circular [9], which can have applications in attoscience [27]. It should be mentioned that Ref. [28] suggested preparing a molecule in a ring-current state with angular momentum $m \neq 0$ by circularly polarized π pulses. HHG from such states can also produce nearly circularly polarized attosecond pulses. In our case such a preparation of the initial state is not necessary, since, in the relevant experiments [6,8], the ground atomic state is the p state and $m \neq 0$ states contribute to the HHG process. In a recently published paper [9] we showed, in an example of a bicircular field having wavelengths of 800 nm and 400 nm, that it is really possible to generate elliptically polarized attosecond pulse trains by using a group of circularly polarized high harmonics. The results obtained in Ref. [9] are based on the general theory which is presented here. In the present paper we show that, for longer bicircular-field wavelengths, the length of the HHG plateau increases so that more harmonics possessing $\varepsilon_n = \pm 1$ asymmetry are available. By combining a group of such harmonics we show that the ratio of the coherent to incoherent sum of the harmonic intensities increases more than twofold for the presently used wavelength of 1300 nm in comparison with the 800-nm-wavelength case from Ref. [9]. In addition to this, the obtained attosecond pulse trains can be shorter than 100 as. We also explored the influence of the relative strength of the bicircular-field components on the HHG spectra and found that, for a stronger 2ω-field component, the plateau and cutoff harmonics are much stronger, while the ellipticity of the corresponding attosecond pulse train is smaller.

The theory introduced in this paper has already been successfully applied to special cases such as are mentioned Ref. [9]. Another application of this theory is given in Ref. [10], where the problem of conservation of spin angular momentum, mentioned in the seminal paper [6], is addressed, and good agreement with the results of [6] is achieved. We hope that our results will be useful for the exploration of chirality sensitive effects in HHG, as well as in other laser-induced processes such as high-order above-threshold ionization [12] and laser-assisted processes such as radiative electron-ion recombination and electron-atom scattering [13,29].

ACKNOWLEDGMENT

We gratefully acknowledge useful discussions with Wilhelm Becker.

APPENDIX A: DYNAMICAL SYMMETRIES AND THE SELECTION RULES

It can be shown analytically that the bicircular field (13) translated in time by $pT/(r+s)$, with p being an integer, is the same as the field rotated by the angle $-pr\phi_{rs}$, $\phi_{rs} = 2\pi/(r+s)$, about the z axis, i.e., that

$$R_z(\alpha)\mathbf{E}(t) = \mathbf{E}\left(t + p\frac{\phi_{rs}}{\omega}\right), \quad \alpha = -pr\phi_{rs}, \tag{A1}$$

where the matrix element of the rotation matrix about the z axis are $[R_z(\alpha)]_{11} = [R_z(\alpha)]_{22} = \cos\alpha$, $[R_z(\alpha)]_{12} = -[R_z(\alpha)]_{21} = \sin\alpha$. Let us act with the unitary rotation operator $D(\alpha) = \exp(-iJ_z\alpha)$, where J_z is the z component of the total angular momentum operator, from the left on the time-dependent Schrödinger equation (2), supposing that $V(\mathbf{r})$ is such that the laser-free Hamiltonian is invariant under rotation by α (for simplicity we consider the one-electron case). In addition, we translate the time-dependent Schrödinger equation in time by $p\phi_{rs}/\omega$. Taking into account that the vector operators transform according to $\mathbf{r}' = D(\alpha)\mathbf{r}D^\dagger(\alpha) = R_z(\alpha)\mathbf{r}$, using Eq. (A1) and the invariance of the scalar product with respect to rotations, we obtain

$$|\Phi_j^{(\pm)}(t)\rangle = D(\alpha)|\Phi_j^{(\pm)}(t + p\phi_{rs}/\omega)\rangle, \quad j = i, f. \tag{A2}$$

Similar results in the context of above-threshold detachment by a bicircular field is obtained in Ref. [11], while for HHG this kind of dynamical symmetry is considered in Ref. [30].

Taking into account relation (A2), for the time-dependent dipole (5) we get (for $p = 0, 1, \ldots, r+s-1$)

$$\begin{aligned}\mathbf{d}_{fi}(t) &= \langle\Phi_f^{(-)}(t)|\mathbf{r}|\Phi_i^{(+)}(t)\rangle \\ &= \langle\Phi_f^{(-)}(t + p\phi_{rs}/\omega)|D^\dagger(\alpha)\mathbf{r}D(\alpha)|\Phi_i^{(+)}(t + p\phi_{rs}/\omega)\rangle \\ &= R_z(-\alpha)\mathbf{d}_{fi}(t + p\phi_{rs}/\omega).\end{aligned} \tag{A3}$$

Equation (7) can be written as

$$\mathbf{T}_n = \sum_{p=0}^{r+s-1} \int_{pT/(r+s)}^{(p+1)T/(r+s)} \frac{dt}{T}\mathbf{d}_{fi}(t)e^{in\omega t}, \tag{A4}$$

so that, after the substitution $t' = t - p\phi_{rs}/\omega$, we obtain

$$\mathbf{T}_n = \sum_{p=0}^{r+s-1} \int_0^{T/(r+s)} \frac{dt'}{T}\mathbf{d}_{fi}(t' + p\phi_{rs}/\omega)e^{in(\omega t' + p\phi_{rs})}. \tag{A5}$$

Applying (A4) for $p = 0, 1, \ldots, r+s-1$ and using

$$\mathbf{T}_{0n} = \int_0^{T/(r+s)} \frac{dt}{T/(r+s)}\mathbf{d}_{fi}(t)e^{in\omega t}, \tag{A6}$$

from (A5), we get

$$\mathbf{T}_n = \sum_{p=0}^{r+s-1} \frac{e^{inp\phi_{rs}}}{r+s} R_z(-pr\phi_{rs})\mathbf{T}_{0n}. \tag{A7}$$

This can be rewritten as

$$T_n^x = T_{0n}^{(+)} S_+ + T_{0n}^{(-)} S_-,\ iT_n^y = T_{0n}^{(+)} S_+ - T_{0n}^{(-)} S_-, \quad \text{(A8)}$$

with q integer, $2T_{0n}^{(\pm)} = T_{0n}^x \pm iT_{0n}^y$, and where the sum

$$S_\pm = \frac{1}{r+s} \sum_{p=0}^{r+s-1} \exp\left(ip2\pi \frac{n \pm r}{r+s}\right) = \delta_{n,q(r+s)\mp r} \quad \text{(A9)}$$

was calculated by using the formula for a geometric series. The ellipticity of the nth harmonic can be expressed through the degree of circular polarization ξ_n [3],

$$\varepsilon_n = \text{sgn}(\xi_n)\left(\frac{1-\sqrt{1-\xi_n^2}}{1+\sqrt{1-\xi_n^2}}\right)^{1/2},$$

$\xi_n = \text{Im}\,(2T_n^{x*}T_n^y)/|T_n|^2$. By using this, for the nth harmonic ellipticity we obtain the selection rule

$$\varepsilon_n = \pm 1 \text{ for } n = q(r+s) \pm r. \quad \text{(A10)}$$

APPENDIX B: VIOLATION OF SELECTION RULES FOR A SPECIFIC CHOICE OF QUANTIZATION AXIS

The result (A10) has to be used with a caution since it is possible that the Hamiltonian $H(t)$ possesses the required symmetry properties, while the laser-free ground-state wave functions $|\psi_j\rangle$ in the boundary conditions (3) violate them. For example, the potential $V(\mathbf{r})$ is spherically symmetric for the inert gases considered here, but the p-ground-state wave function is not. If we choose the quantization axis to be the z axis then the ground-state wave function is symmetric with respect to rotation around the z axis. In this case the result (A10) can be applied. For other choices of quantization axis it is violated. If there is a preferred axis [for example, the axis determined by an additional (external) static field or internuclear axis of an aligned diatomic molecule], then the results depend on the choice of the quantization axis. The influence of the orientation of quantization axis was analyzed in Ref. [31], where geometrical aspects of ionization from aligned quantum states were investigated. In a similar vein, we can fix the quantization axis and the initial and final states in order to see how this choice affects the HHG spectrum and the selection rules.

Let us suppose that we have a closed shell and the p ground state, but that the quantization axis is along the x axis. Let us also suppose that $m_i = m_f = 0$. In this case, the method, introduced in Sec. III, with the calculation of ΔJ_z cannot be directly applied. Namely, the wave vectors of the harmonic and laser fields are along the z axis, while the p ground state is characterized with the quantization axis along the x axis and the corresponding momentum-space wave function is proportional to $Y_{10}(\theta_q, \phi_q = 0)$. We have to rotate this spherical harmonic by using the Wigner rotation matrices and express

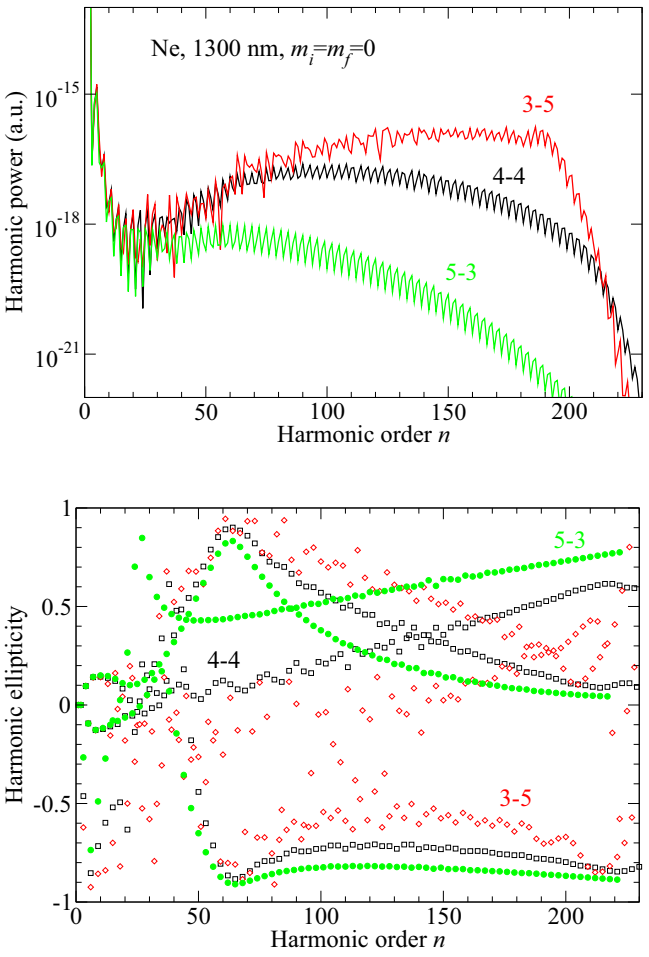

FIG. 5. (Color online) Harmonic power (upper panel) and ellipticity (lower panel) as functions of the harmonic order for HHG by the same field as in Fig. 1 and for Ne atoms with the $2p$ ground state but for the x axis as axis of quantization and for $m_i = m_f = 0$.

it via Y_{1m}, $m = 0 \pm 1$, in the system with the z quantization axis. Then, for new Y_{1m} (which are now with respect to the z axis) we can apply the selection rule (14). Only the matrix elements with $m = \pm 1$ survive and we obtain the selection rule (19) (which was previously developed for open shells, while it is now for closed shells and the x quantization axis). This selection rule is proved by numerical calculations [we calculated the double integral over the times t and τ, Eqs. (7) and (10), with the matrix element given in analytical form for Ne atoms and the quantization in the direction of the x axis]. Let us show, by using an example, that, in this case, the emitted harmonics do not have to be circularly polarized. From the upper panel of Fig. 5, we see that all harmonics $n = 1,2,3,\ldots$ are emitted, while from the lower panel we see that these harmonics are elliptically polarized.

[1] H. Eichmann, A. Egbert, S. Nolte, C. Momma, B. Wellegehausen, W. Becker, S. Long, and J. K. McIver, Phys. Rev. A **51**, R3414 (1995).

[2] S. Long, W. Becker, and J. K. McIver, Phys. Rev. A **52**, 2262 (1995).

[3] D. B. Milošević, W. Becker, and R. Kopold, Phys. Rev. A **61**, 063403 (2000); D. B. Milošević and W. Sandner, Opt. Lett. **25**, 1532 (2000); D. B. Milošević, W. Becker, R. Kopold, and W. Sandner, Laser Phys. **11**, 165 (2001).

[4] D. B. Milošević, W. Becker, and R. Kopold, in *Atoms, Molecules and Quantum Dots in Laser Fields: Fundamental Processes*, edited by N. Bloembergen, N. Rahman, and A. Rizzo (Società Italiana di Fisica, Bologna, 2001), Vol. 71, pp. 239–252.
[5] D. B. Milošević and W. Becker, Phys. Rev. A **62**, 011403(R) (2000); J. Mod. Opt. **52**, 233 (2005).
[6] A. Fleischer, O. Kfir, T. Diskin, P. Sidorenko, and O. Cohen, Nat. Photonics **8**, 543 (2014).
[7] E. Pisanty, S. Sukiasyan, and M. Ivanov, Phys. Rev. A **90**, 043829 (2014).
[8] O. Kfir *et al.*, Nat. Photonics **9**, 99 (2015).
[9] D. B. Milošević, Opt. Lett. **40**, 2381 (2015).
[10] D. B. Milošević, J. Phys. B: At., Mol. Opt. Phys. **48**, 171001 (2015).
[11] E. Hasović, D. B. Milošević, and W. Becker, Laser Phys. Lett. **3**, 200 (2006); A. Kramo, E. Hasović, D. B. Milošević, and W. Becker, *ibid.* **4**, 279 (2007); E. Hasović, A. Kramo, and D. B. Milošević, Eur. Phys. J. Spec. Top. **160**, 205 (2008).
[12] C. A. Mancuso *et al.*, Phys. Rev. A **91**, 031402(R) (2015).
[13] D. B. Milošević and F. Ehlotzky, Adv. At. Mol. Opt. Phys. **49**, 373 (2003).
[14] M. Kohler, T. Pfeifer, K. Hatsagortsyan, and C. Keitel, Adv. At. Mol. Opt. Phys. **61**, 159 (2012).
[15] P. B. Corkum, Phys. Rev. Lett. **71**, 1994 (1993).
[16] K. C. Kulander, K. J. Schafer, and J. K. Krause, in *Atoms in Intense Laser Fields*, edited by M. Gavrila (Academic, New York, 1992), pp. 247–300.
[17] A. A. Radzig and B. M. Smirnov, *Reference Data on Atoms, Molecules and Ions* (Springer, Berlin, 1985).
[18] M. E. Rose, *Elementary Theory of Angular Momentum* (Dover, New York, 1995).
[19] Process in which the initial and final electron states are substates differing only in the magnetic quantum number was called degenerate combinational harmonic generation in V. N. Ostrovsky and J. B. Greenwood, J. Phys. B **38**, 1867 (2005); V. N. Ostrovsky, *ibid.* **38**, 4399 (2005).
[20] W. Becker, F. Grasbon, R. Kopold, D. B. Milošević, G. G. Paulus, and H. Walther, Adv. At. Mol. Opt. Phys. **48**, 35 (2002).
[21] This is the reason why the HHG by bicircular fields is very efficient. Notice also that the ionization happens near a maximum of the electric-field amplitude.
[22] In comparison with the classical three-step model [15], mentioned in Sec. II, the main feature of our semiclassical three-step model is that the (ionized) electron starts on its orbit with nonzero complex velocity whose value is determined by the condition that it returns to the origin. It can be shown that the probability of the HHG process is smaller for larger value of the electron velocity at the ionization time [3].
[23] I. Barth and J. Manz, Phys. Rev. A **75**, 012510 (2007).
[24] I. Barth and O. Smirnova, Phys. Rev. A **84**, 063415 (2011).
[25] N. Böwering, T. Lischke, B. Schmidtke, N. Müller, T. Khalil, and U. Heinzmann, Phys. Rev. Lett. **86**, 1187 (2001); M. H. M. Janssen and I. Powis, Phys. Chem. Chem. Phys. **16**, 856 (2014).
[26] J. Stöhr *et al.*, Science **259**, 658 (1993); *Magnetism and Synchrotron Radiation: New Trends*, edited by E. Beaurepaire, H. Bulou, F. Scheurer, and J. P. Kappler (Springer, Heidelberg, 2010).
[27] P. Agostini and L. F. DiMauro, Rep. Prog. Phys. **67**, 813 (2004); F. Krausz and M. Ivanov, Rev. Mod. Phys. **81**, 163 (2009).
[28] X. Xie, A. Scrinzi, M. Wickenhauser, A. Baltuška, I. Barth, and M. Kitzler, Phys. Rev. Lett. **101**, 033901 (2008).
[29] D. B. Milošević, D. Bauer, and W. Becker, J. Mod. Opt. **53**, 125 (2006).
[30] O. E. Alon, V. Averbukh, and N. Moiseyev, Phys. Rev. Lett. **80**, 3743 (1998); F. Ceccherini, D. Bauer, and F. Cornolti, J. Phys. B. **34**, 5017 (2001).
[31] T. Birkeland, M. Førre, J. P. Hansen, and S. Selstø, J. Phys. B: At., Mol. Opt. Phys. **37**, 4205 (2004).